World Academy of Science, Engineering and Technology
International Journal of Aerospace and Mechanical Engineering
Vol:3, No:3, 2009

Mixed Convection in a 2D-channel with a Co-Flowing Fluid Injection: Influence of the Jet Position

Ameni Mokni, Hatem Mhiri , Georges Le Palec , And Philippe Bournot

***Abstract*—**Numerical study of a plane jet occurring in a vertical heated channel is carried out. The aim is to explore the influence of the forced flow, issued from a flat nozzle located in the entry section of a channel, on the up-going fluid along the channel walls. The Reynolds number based on the nozzle width and the jet velocity ranges between 3 10^3 and 2.10^4; whereas, the Grashof number based on the channel length and the wall temperature difference is 2.57 10^{10}. Computations are established for a symmetrically heated channel and various nozzle positions. The system of governing equations is solved with a finite volumes method. The obtained results show that the jet-wall interactions activate the heat transfer, the position variation modifies the heat transfer especially for low Reynolds numbers: the heat transfer is enhanced for the adjacent wall; however it is decreased for the opposite one. The numerical velocity and temperature fields are post-processed to compute the quantities of engineering interest such as the induced mass flow rate, and the Nusselt number along the plates.

***Keywords*—**Channel, Heat flux, Jet, Mixed convection.

I. Introduction

NATURAL convection is unquestionably regarded as a very attractive mode of cooling because of its little cost, minimal maintenance and low noise [1]. Natural convection between heated vertical parallel plates is the most frequently used configuration in convection air cooling of electronic equipment. The passive character of cooling by natural convection makes it very attractive for applications in electronic devices. However, in order to increase the cooling requirements, researches for methods to improve the heat transfer parameters or to analyze standard configurations to carry out optimal geometrical parameters for a better heat transfer rate [2]–[9]. Adding a forced convection flow is a solution to enhance heat transfer.

In many applications although forced convection heat transfer is involved, the effect of buoyancy is not negligible. Such flows are known as mixed convection flows. When the Reynolds number (Re) or the Grashof number (Gr) is high enough, the flow become turbulent.

Pioneering work on turbulent mixed convection particularly from vertical tubes has been done by Jackson and co-workers [10]–[12]. Nakajima et al. [13] studied the effect of buoyancy on the turbulent transport processes in mixed convection for both aiding and opposing flows. Correlations for dimensionless mass flow rate, maximum wall temperature and average Nusselt number, in terms of Rayleigh number and dimensionless geometric parameters are presented by several authors in order to compute the quantities of engineering interest [14]-[21]: we can cite Penot and al. [20] who proposed useful correlations to determine the flow rate, the fluid temperature, and the Nusselt number according to the heat flux density, the pressure difference and the Reynolds and Grashof numbers. M. Najam et al. [21] studied numerically the mixed convection in a "T" form cavity heated with a constant heat flux and subjected to an air blast entering by the bottom. They showed the competition between natural and forced convection. The heat transfer was found maximal in the zone where the role of natural convection is more significant.

The present theoretical study is concerned with mixed convection in asymmetrically heated vertical channel submitted to a vertical jet of fresh air entering by the bottom. Numerical results are presented in terms of dimensionless induced mass flow rates and dimensionless wall temperatures for a Rayleigh number Ra= 2.57 10^{10} based on the heat transfer and the channel length and different Reynolds numbers. Moreover, Nusselt numbers varying with the dimensionless axial coordinate X pave the way for the calculation of the average Nusselt numbers. Computations are established for a symmetrically heated channel and various jet positions. Some optimal geometrical configurations have been identified corresponding to the maximum average Nusselt number.

II. Assumptions and Governing Equations

A computational domain of finite dimension illustrated in Fig. 1 is employed to simulate the vertical channel. A gas jet is issued from a flat nozzle located at various position at the bottom of the channel. The chimney walls are subject to a constant heat flux. Numerical results are reported for dry air

A. Mokni is with the IUSTI UMR CNRS 6595, Technopole de Chateau-Gombert, 5 rue Enrico Fermi, 13013 Marseille Cedex 20 – France and with Unité de Thermique et Environnement, Ecole Nationale d'Ingénieurs de Monastir, Route de Ouardanine 5000 MONASTIR (TUNISIA) (phone: (+216) 97228560; e-mail: ameni26@yahoo.fr).

H. Mhiri, Jr., is with Unité de Thermique et Environnement, Ecole Nationale d'Ingénieurs de Monastir, Route de Ouardanine 5000 MONASTIR (TUNISIA)

G. Le Palec is with IUSTI UMR CNRS 6595, Technopole de Chateau-Gombert, 5 rue Enrico Fermi, 13013 Marseille Cedex 20 – France

Ph. Bournot is with IUSTI UMR CNRS 6595, Technopole de Chateau-Gombert, 5 rue Enrico Fermi, 13013 Marseille Cedex 20 – France

as coolant. The unconfined airflow lies far away from the region of the disturbance induced by the presence of the jet flow. The channel is long enough that the flow becomes turbulent before the exit. The influence of this forced additional jet is analyzed by using the low Reynolds number k-ε turbulence model. Mixed convection is considered by using the Boussinesq approximation in which the density varies linearly with temperature. Other thermo-physical quantities are assumed to be constant. The flow is assumed steady and incompressible.

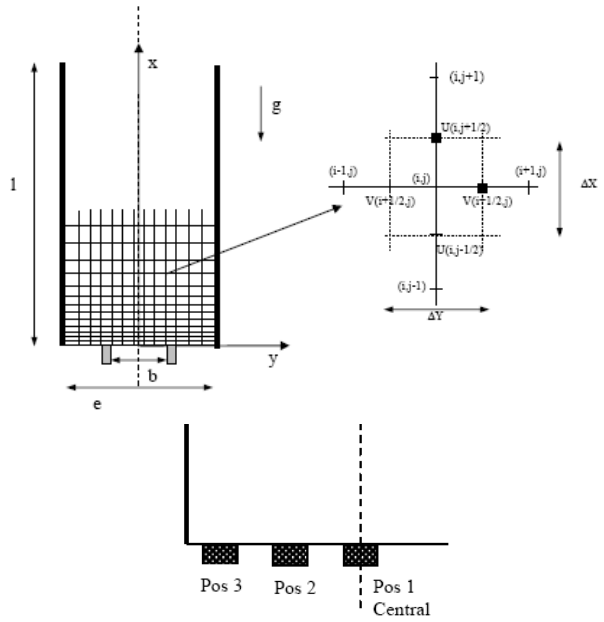

Fig.1 Coordinate system of the configuration flow

Dimensionless variables are defined by:

$$X=\frac{x}{L},\ Y=\frac{y}{L},\ U=\frac{u}{u_0},\ V=\frac{v}{u_0},\ P=\frac{(p+\rho gx)e^2}{\rho\alpha^2},$$

$$\theta=\frac{T-T_\infty}{\phi H}\lambda,\ K=\frac{ke^2}{\alpha^2}\ \text{et}\quad E=\frac{\varepsilon e^4}{\alpha^3} \tag{1}$$

The dimensionless governing equations for two dimensional buoyancy–driven flows, with no viscous dissipation, can be written as follows:

Continuity equation:

$$\frac{\partial U}{\partial X}+\frac{\partial V}{\partial X}=0 \tag{2}$$

Momentum equation in X direction:

TABLE I
NOMENCLATURE

Symbol	Quantity	units
b	Width of the nozzle exit	m
C_f	Friction coefficient $C_f=\frac{2\tau_p}{\rho u_m^2}$	
e	Width of the channel	m
E	Dimensionless dissipation rate of turbulent kinetic energy	
g	gravitational acceleration	ms-2
Gr	Grashof number $Gr=\frac{g\beta\varphi H^4}{\nu^2\lambda}$	
h	Local heat transfer coefficient	$Wm^{-2}K^{-1}$
k	Turbulent kinetic energy	m^2s^{-2}
K	Dimensionless turbulent kinetic energy	
ℓ	length of the heated vertical plates	m
L	Dimensionless length of the heated vertical plate	
Nu_m	Average Nusselt number	
Nu_x	Local Nusselt number $Nu_x=\frac{h_x l}{\lambda}$	
Pos	Nozzle position	
Pr	Prandtl number $\Pr=\frac{\upsilon}{\alpha}$	
Q_1	Dimensionless mass flow rate at the inlet section of the channel	
Q_2	Dimensionless mass flow rate at the exit section of the nozzle	
Ra	Average Rayleigh number $\mathrm{Ra}=\frac{g\beta H^4\varphi}{\lambda\alpha\upsilon}=\mathrm{Gr.Pr}$	
Ra_x	Local Rayleigh number $Ra=\frac{g\beta x^4\varphi}{\lambda\alpha\upsilon}$	
Re	Reynolds number $\mathrm{Re}=\frac{bu_0}{\upsilon}$	
T	temperature	k
u,v	components of velocity, respectively	ms^{-1}
U,V	dimensionless components of velocity, respectively	
x,y	coordinates, respectively	m
X,Y	dimensionless coordinates, respectively	
α	thermal diffusivity of the fluid	m^2s^{-1}
ε	Rate of dissipation of turbulent kinetic energy	m^2s
β	coefficient of thermal expansion	k^{-1}
θ	dimensionless temperature	
λ	thermal conductivity of the fluid	$W\,m^{-1}k^{-1}$
υ	kinematic viscosity	m^2s^{-1}
ρ	fluid density	$kg\,m^{-3}$
τ	Wall shear stress $\tau=\mu\left(\frac{\partial u}{\partial y}\right)_{y=0}$	Pa
ϕ	Wall heat flux	Wm^{-2}

$$U\frac{\partial U}{\partial X}+V\frac{\partial U}{\partial Y}=-\frac{\partial P}{\partial X}+(\mathrm{Pr}+\mathrm{Pr}_t)\left[\frac{\partial^2 U}{\partial X^2}+\frac{\partial^2 U}{\partial Y^2}\right]-\frac{2}{3}\frac{\partial K}{\partial X}+Ra\,\mathrm{Pr}\,\theta \tag{3}$$

Momentum equation in Y direction:

$$U\frac{\partial V}{\partial X}+V\frac{\partial V}{\partial Y}=-\frac{\partial P}{\partial Y}+(\mathrm{Pr}+\mathrm{Pr}_t)\left[\frac{\partial^2 V}{\partial X^2}+\frac{\partial^2 V}{\partial Y^2}\right]-\frac{2}{3}\frac{\partial K}{\partial Y} \tag{4}$$

Energy equation:

$$U\frac{\partial\theta}{\partial X}+V\frac{\partial\theta}{\partial Y}=2\left[\frac{\partial^2\theta}{\partial X^2}+\frac{\partial^2\theta}{\partial Y^2}\right] \quad (5)$$

Turbulent kinetic energy equation:

$$U\frac{\partial K}{\partial X}+V\frac{\partial K}{\partial Y}=(\mathrm{Pr}+\frac{\mathrm{Pr}_t}{\sigma_k})(\frac{\partial^2 K}{\partial X^2}+\frac{\partial^2 K}{\partial Y^2})-E+G_{DK}+G_{DB} \quad (6)$$

Rate of dissipation of turbulent kinetic energy equation:

$$\mathrm{U}\frac{\partial \mathrm{E}}{\partial \mathrm{X}}+\mathrm{V}\frac{\partial \mathrm{E}}{\partial \mathrm{Y}}=(\mathrm{Pr}+\frac{\mathrm{Pr_t}}{\sigma_\varepsilon})(\frac{\partial^2 \mathrm{E}}{\partial \mathrm{X}^2}+\frac{\partial^2 \mathrm{E}}{\partial \mathrm{Y}^2})-\mathrm{C}_1\frac{\mathrm{E}}{\mathrm{K}}\mathrm{G}_D+C_2\frac{E^2}{K} \quad (7)$$

Where:

$$G_{DK}=\mathrm{Pr}_t(\frac{\partial U_i}{\partial X_j}+\frac{\partial U_j}{\partial X_i})\frac{\partial U_i}{\partial X_j}-\frac{2}{3}K\delta_{ij}\frac{\partial U_i}{\partial X_j}$$

and

$$G_{DB}=\frac{1}{Fr}\frac{\nu_t}{\mathrm{Pr}_t}\frac{\partial\theta}{\partial X} \quad (8)$$

E stands for the turbulent kinetic energy production due to shear, while G_{DK} is the turbulent kinetic energy production due to the mean velocity gradients, and G_{DB} is the turbulent kinetic energy production due to the buoyancy.

The standard k-ε model is used, so that constants are those given by Jones and Lauder [21]: $C_1=1.44$; $C_2=1.92$; $C_3=0.7$; $C_\mu=0.09$; $\sigma_\varepsilon=1.0$; $\sigma_k=1.30$; $\mathrm{Pr_t}=1.0$.

The boundary conditions are the following:

At $Y=-\frac{e}{2L}$; $U=0$; $V=0$; $\left(\frac{\partial\theta}{\partial Y}\right)_p=1$, $K=0$,

At $Y=\frac{e}{2L}$; $U=0$; $V=0$; $\left(\frac{\partial\theta}{\partial Y}\right)_p=1$, $K=0$,

At $X=0$;

$$-\frac{e}{2L}<Y<-\frac{b}{2L}\ ;\ \frac{\partial U}{\partial X}=0\ ,\ V=0\ ,\ P_g=-\frac{Q_1^2}{2}\ ,\ \theta=0\ ,\ K=\frac{3}{2}I_tU^2$$

$$-\frac{b}{2L}<Y<\frac{b}{2L}\ ;\ U=1\ ,\ V=0\ ,\ \theta=0\ ,\ K=0.001 \quad (9)$$

$$\frac{b}{2L}<Y<\frac{e}{2L}\ ;$$

$$\frac{\partial U}{\partial X}=0\ ,\ V=0\ ,\ P_g=-\frac{Q_1^2}{2}\ ,\ \theta=0\ ,\ K=\frac{3}{2}I_tU^2$$

At $X=1$; $\frac{\partial U}{\partial X}=\frac{\partial V}{\partial X}=\frac{\partial\theta}{\partial X}=0$, $P=0$, $K=\frac{3}{2}I_tU^2$, $E=\frac{2e\,K^{0.5}}{b}$

where $Q_1=\int_{b/2L}^{e/2L} U dY=\int_{-e/2L}^{-b/2L} U dY$

and $Q_2=\int_{-b/2L}^{b/2L} U dY$.

I_t is the turbulence intensity.

III. NUMERICAL RESULTS

The Results of the present investigation are carried out for air, Pr = 0.71, the Rayleigh number based on the channel length range is 2.5710^{10}, the Reynolds number based on the jet velocity ranges between 3 10^3 and 2 10^4. We study the influence of the velocity and the position of the jet on the heat transfer enhancement. Computations deals with a symmetrically heated channel.

For purpose of validation, the computations were performed first for a simple channel - i.e. without gas injection from the nozzle - and numerical results were compared with the experimental ones published by A. Auletta et al. [22]. The local Nusselt defined by $Nu=\frac{\phi(x)x}{(T_p(x)-T_\infty)\lambda}$ is reported in figure 2. The resulting free convection problem was simulated with L/e =2.5 which corresponds to a Rayleigh number equal to 1.16 10^{11}. The Prandtl number is 0.71 (air).

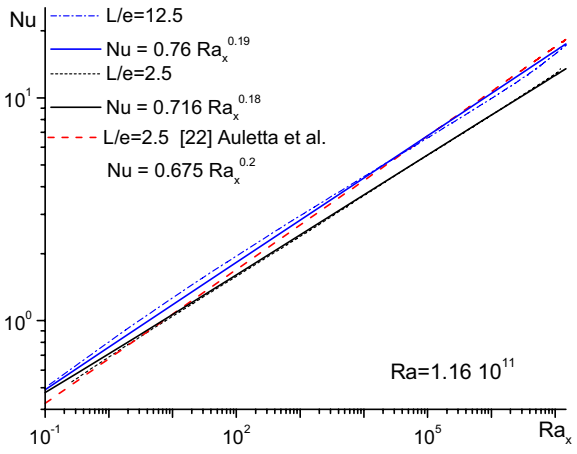

Fig. 2. Local Nusselt number variation according to the local Rayleigh number. Natural convection flow Comparison with experiments.

Differences between measurements and numerical predictions are very low and they mainly concern the highest part of the channel. This may be due to the fact that there were some heat losses caused by insufficient thermal insulation in

experiments. Moreover, the imposed wall heat flux was not uniform because of the space between two successive heaters. At least, the use of thermocouples also modifies the flow structure, especially in the vicinity of the plates.

The study is carried out for a constant channel geometrical characteristics L/e =12.5. We notice, for this aspect ratio, a linear increase of the local wall Nusselt number according the relation:

$$Nu = 0.76 Ra_x^{0.19} \qquad (10)$$

A. Mass flow rate

Note that the introduction of the disturbance at the channel entrance activates the convection flow; the natural convection flow increases according the jet velocity; indeed the natural convection flow is higher in presence of the jet. The buoyancy influence is noticeable for low Reynolds numbers, so it has a significant impact on the driven flow. In contrast to height Reynolds numbers, the flow is mainly driven by the mean pressure gradient, so it increases according the jet velocity.

The natural convection flow is independent also, of the nozzle position for low values of Reynolds number. A notable dependence on the nozzle position starts to be seen gradually from Re=5000. The difference is noted between the central position and the two others. Induced mass flow rate is almost the same for the two shifted positions.

The mass flow rate on both sides of the jet involves according to the following correlation for a jet Reynolds number Re> 3. 10^3:

For central position: $Q = 2Q_1 = -11158 + 30.1\,\mathrm{Re}$ (11)

For shifted positions: $Q = 2Q_1 = -9366 + 33.6\,\mathrm{Re}$ (12)

The flow structure is, essentially, composed of the open lines, which represent the forced flow, and closed cells which are due to the recirculation movement up of the jet or to natural convection phenomena (Fig.4.). The thermal gradient which exists between the fluid and the hot walls will cause a vertical aspiration of air with a non-negligible mass flow rate. The vertical jet of fresh air entering by the bottom of the heated channel interacts with the heated walls. As the Reynolds number increases, the jet interacts with the walls more and more far from the nozzle.

This impact causes, in addition of the coldest zones; the formation of a rotating cell with weak intensity behind the impact zone, because it opposes to buoyancy forces. These rotating cells do not support heat transfer and generate the formation of hot zones.

These zones move towards the exit section of the channel. For the two shifted positions the symmetry breaks down, the jet interacts with the opposite wall more and more far from the nozzle. The swirling size increases and constrains the jet of forced flow to pass close to this plane. In the other hand, the jet pass close to the adjacent wall; more the jet is closer to the wall, more the impact zone is closer to the entrance section, more it penetrates into the cavity.

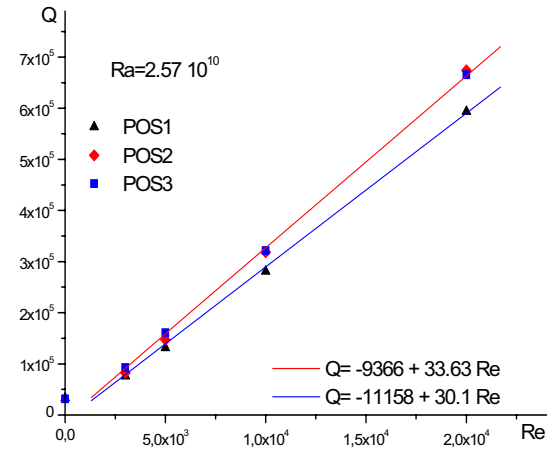

Fig. 3. Natural convection and driven flow rate in the entrance section according to the Reynolds number

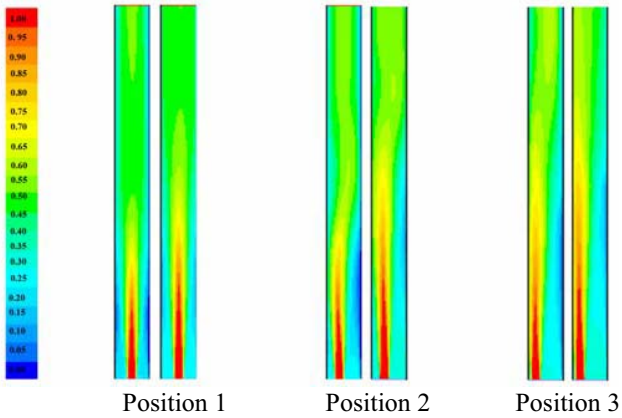

Fig. 5. Streamlines for different jet position Ra=2.57 10^{10}, Re=310^3 (right), Re=210^4 (left)

B. Skin friction

The skin friction coefficient $C_f = \frac{2\tau_p}{\rho u_0^2}$ is plotted on figure 5.

For all the treated cases, note that the two walls behave in the same manner for the central position; however they operate in an opposite way for the two shifted positions.

The skin friction decreases from the leading edge. A peak is noticed, further, located on the impact zone. The skin friction maximum on the adjacent wall, correspond to the minimum on the opposite wall and vice versa.

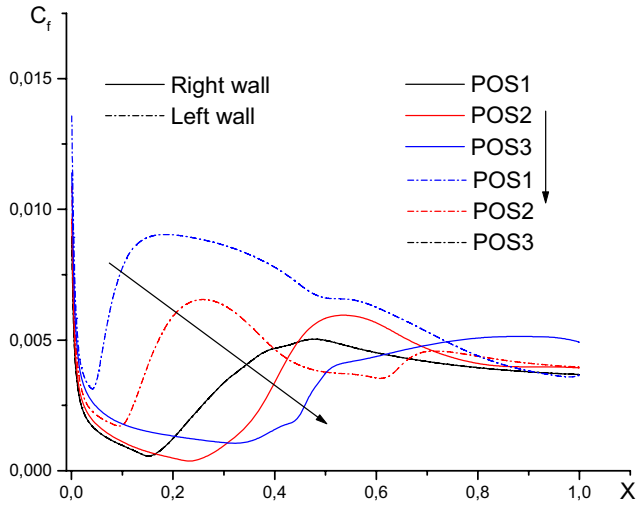

(a). Re = 3. 10^3

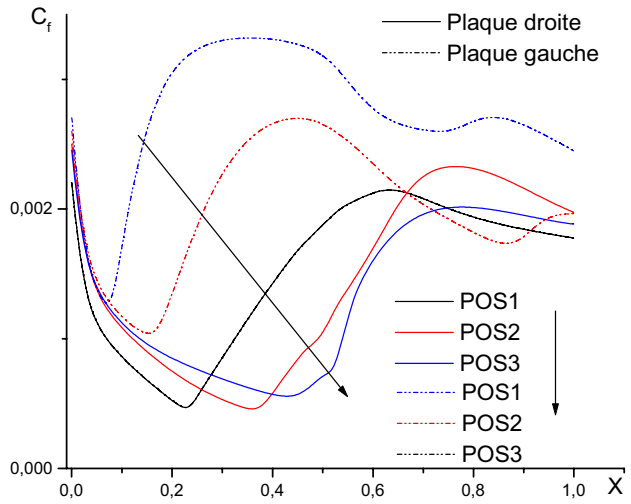

Fig. 5. streamwise evolution of the local friction coefficient (b). Re = 2. 10^4

C. Local Nusselt number

Fig. 6 illustrates the Nusselt number values as a function of the longitudinal X coordinate for different nozzle position, at Ra= 2.57 10^{10} for Re=310^3 in Fig.6 (a) and Re=210^4 in Fig. 6(b). The Nusselt number values are higher for the adjacent wall; this trend is due to the greater mass flow rate induced by the jet allowing a better heat transfer activity. The heat transfer decreases gradually from the inlet section. For lowest Reynolds numbers, the minimum heat transfer zones on the opposite wall are larger for the more shifted nozzle.

For high Reynolds numbers, a weak difference is signaled for the ratio $Nu_x / \mathrm{Re}_x^{0.5}$ and concerns especially the impact zone.

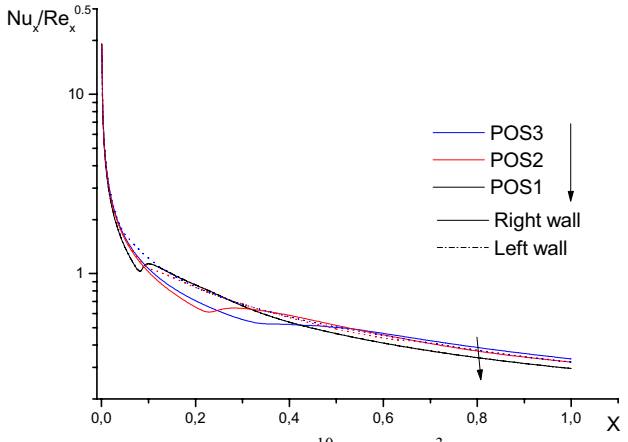

(a). Ra = 2.5710^{10} Re= 3 10^3

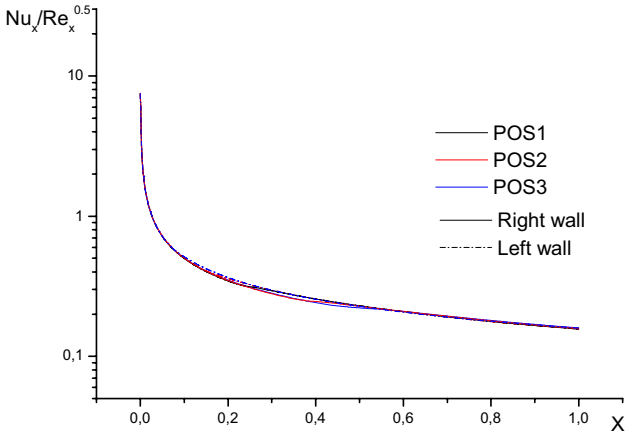

(b). Ra = 2.5710^{10} Re=2 10^4

Fig. 6. Local Nusselt number for various jet positions

D. Average Nusselt number

In order to better quantify the total heat transfer between the channel and the flow, let us introduce the average Nusselt number, defined as:

$$Nu_m = \overline{Nu} = \frac{\overline{h} L}{\lambda} \qquad \text{where}$$

$$\overline{h} = \frac{1}{l}\int_0^l h_x dx = \frac{1}{l}\int_0^l \frac{\phi}{T_p(x) - T_\infty} dx \qquad (13)$$

The average Nusselt number is plotted according the jet Reynolds number on Figure 7. We notice that the average Nusselt number increases according to the Reynolds number for both channel walls, which can to be explained by fact that the thickness of the boundary layer, which acts as a heat insulator, decreases when the Reynolds number increases.

It follows that the convective exchange between the flow and the heated walls increases. Fig.7. shows also a little increase of the channel Nusselt number according to shifted position for low Reynolds numbers. Indeed for these cases the heat transfer enhancement of the adjacent plate is larger than the decrease of the opposite one. A weak increase of the total channel Nusselt number is noted.

For high Reynolds numbers the average heat transfer is

unchanged even when we change the nozzle position. Predictable results since the heat transfer is almost the same for high Reynolds numbers (Fig.6.b). This can be explained by the fact that the induced mass flow rate ensures the maximum exchange.

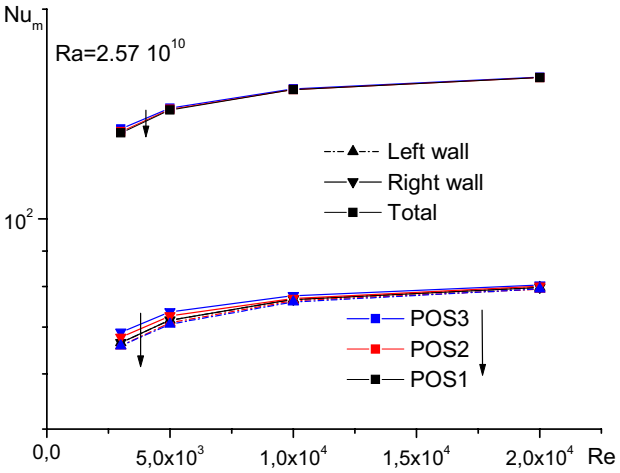

Fig.7. Evolution of the average Nusselt number

IV. Conclusion

A numerical study of both natural and mixed convection in a 2D-channel submitted to a constant wall heat flux was performed. The mixed flow is obtained by using an ascending jet located at the entry section of the channel. Computations were performed for Ra=2.57 1010, Reynolds number ranging between 3 103 and 2104 and three nozzle positions. The numerical procedure was validated by comparing our results with the experimental ones by Auletta [22]. Special attention has been carried to the thermal behaviour of the flow, especially the influence of the jet position on the heat transfer. The mass flow rate induced increases according to the Reynolds number. The nozzle position affects the induced mass flow rate for important Reynolds numbers. The difference is noted only between the central position and the two others shifted.

The vertical jet at the entrance permits good ventilation the cavity and then it's favourable to heat exchange from the cavity towards the exterior. It was shown that for high Reynolds number, the flow field is mainly controlled by the external flow and heat transfer is almost similar for all the considered positions. The mean influence concerns the lowest Reynolds numbers: The heat transfer is enhanced for the adjacent wall; however it is decreased for the opposite one. The total Nusselt number is weakly increased.

References

[1] O. Manca, B. Morrone, S. Nardini, V. Naso, Natural convection in open channels, in: B. Sunden, G. Comini (Eds.), Computational Analysis of Convection Heat Transfer, WIT Press, Southampton, UK, 2000, pp. 235– 278.

[2] S.J. Kim, S.W. Lee, Air Cooling Technology for Electronic Equipment, CRC Press, Boca Raton, FL, 1996.

[3] A. Bejan, Shape and Structure from Engineering to Nature, Cambridge University Press, New York, 2000.

[4] G.A. Ledezma, A. Bejan, Optimal geometric arrangement of staggered vertical plates in natural convection, ASME J. Heat Transfer 119 (1997) 700–708.

[5] S. Sathe, B. Sammakia, A review of recent developments in some practical aspects of air-cooled electronic packages, ASME J. Heat Transfer 120 (1998) 830–839.

[6] A. Bejan, A.K. da Silva, S. Lorente, Maximal heat transfer density in vertical morphing channels with natural convection, Numer. Heat Transfer A 45 (2004) 135–152.

[7] A. Auletta, O.Manca, B. Morrone, V. Naso, Heat transfer enhancement by the chimney effect in a vertical isoflux channel, Int. J. Heat Mass Transfer 44 (2001) 4345–4357.

[8] A.K. da Silva, L. Gosselin, Optimal geometry of L- and C-shaped channels for maximum heat transfer rate in natural convection, Int. J. Heat Mass Transfer 48 (2005) 609–620.

[9] A. Andreozzi, A. Campo, O. Manca, Compounded natural convection enhancement in a vertical parallel-plate channel, Int. J. Thermal Sciences 47 (6) (2008) 742–748.

[10] W.B. Hall, J.D. Jackson, Laminarization of a turbulent pipe flow by buoyancy forces, ASME paper, ASME paper no. 69-HT-55 (1969).

[11] J.D. Jackson, W.B. Hall, Influence of buoyancy on heat transfer to fluids flowing in vertical tubes under turbulent conditions, in: S. Kakac, D.B. Spalding (Eds.), Turbulent Forced Convection in Channels and Bundles,Hemisphere Publishing, USA, 1979, pp. 613–640.

[12] Jiulei Wang, Jiankang Li, J.D. Jackson, A study of the influence of buoyancy on turbulent flow in a vertical plane passage, Int. J. Heat Fluid Flow 25 (2004) 420–430.

[13] K. Nakajima, K. Fukui, H. Ueda, T. Mizushina, Buoyancy effects on turbulent transport in combined free and forced convection between verticalparallel plates, Int. J. Heat Mass Transfer 23 (1980) 1325–1336.

[14] M. Miyamoto, Y. Katoh, J. Kurima, H. Saki, Turbulent free convection heat transfer from vertical parallel plates. In Heat Transfer, Vol. 4. (eds C. L. Tien, V. P.Carey and J. K. Ferrell) Hemisphere, Washington DC, 1986, pp. 1593- l598.

[15] A. Auletta, O. Manca, Heat and fluid flow resulting from the chimney effect in a symmetrically heated vertical channel with adiabatic extensions, International Journal of Thermal Sciences, 41 (2002), pp. 1101–1111.

[16] A.G. Fedorov and R.Vskanta, Turbulent natural convection heat transfer in an asymmetrically heated vertical parallel plate channel; International Journal of Heat Mass Transfer, 40 (1997), 16, pp. 3849-3860.

[17] T.A.M. Versteegh, F.T.M. Nieuwstadt., Turbulent budgets of natural convection in an infinite, differentially heated, vertical channel. International Journal of Heat and Fluid Flow, 19 (1998), pp.135-149.

[18] T.A.M. Versteegh, F.T.M. Nieuwstadt., A direct numerical simulation of natural convection between two infinite vertical differentially heated walls scaling laws and wall functions, International Journal of Heat and Mass Transfer, 42 (1999), pp.3673-3693.

[19] A.M. Dalbert, F.Penot, JL.Peube, convection naturelle laminaire dans un canal vertical chauffé à flux constant, International Journal of Heat and Mass Transfer, 24 (1981), 9, pp. 1463-1473.

[20] F. Penot, A.M.Dalbert, convection naturelle mixte et forcée dans un thermosiphon vertical chauffé à flux constant, International Journal of Heat and Mass Transfer,.26 (1983), 11, pp. 1639-1647.

[21] M. Najam, M. El Almi, M. Hasnaoui, A. Amahamid, Etude numérique de la convection mixte dans une cavité en forme de T soumis à un flux de chaleur constant et ventilé par le bas à l'aide d' un jet d'air vertical, Compte Rendu de Mecanique 330 (2002) 461-467.

[22] A. Auletta, O. Manca, Heat and fluid flow resulting from the chimney effect in a symmetrically heated vertical channel with adiabatic extensions, International Journal of Thermal Sciences 41 (2002) 1101–1111